



SYNTHESIS, CHARACTERIZATION, ANTIBACTERIAL ACTIVITIES AND MOLECULAR DOCKING STUDIES OF SOME NOVEL THERAPEUTIC, *N,N*-DISUBSTITUTED β -BRANCHED NITROOLEFIN PIPERAZINE DERIVATIVES

J. IRSHAD AHAMED¹ AND K. S. MEENA*

^{1*} *Bioinformatics Infrastructure Facility Center and Department of Chemistry, Queen Mary's College University of Madras, Chennai, Tamil Nadu, India.*

ABSTRACT

Piperazines are a wide class of chemical compounds with numerous important pharmacological properties. An ease and highly efficient synthetic protocol was accomplished for the synthesis of novel *N,N*-disubstituted β -branched nitroolefin containing new piperazine molecular architectures. As the Michael addition of alkyl anion equivalents to simple nitro olefins proceeds in a non-stereo selective way, the lofty stereo selectivity requires heteroatom substituent on the β - position of the nitronated anion intermediates. Eleven new *N,N*-disubstituted β -branched nitroolefin piperazine derivatives were synthesized using this technique, purity of compounds was ascertained by melting point and thin-layer chromatography. All Compounds have been characterized by ¹H–¹³C NMR. Among the synthesized new compound 10g 1,4-bis((*E*)-3-(3,4-dimethoxyphenyl)-2-nitroallyl) piperazine exhibited potent antimicrobial activities by both Disc diffusion and broth dilution method. The synthesized compounds were subjected to molecular docking studies through commercial software using Discovery Studio 4.0. Furtherly the pharmacokinetics properties were studied by ADMET (Absorption, Distribution, Metabolism, Excretion, Toxicity). DMol³ Properties and B3LYP functions were executed in DFT (Density Functional Theory studies) DS 4.0. The compound 10g was found to be a potent and safe by ADMET studies. The compound 10g could be proposed for further in vitro and in vivo studies.

KEYWORDS: 1, 4-disubstituted piperazines synthesis, molecular docking, Gram(+) bacteria, Gram(-) bacteria, Disc Diffusion Method, MIC (μ g/ml).



K. S. MEENA*

Bioinformatics Infrastructure Facility Center and Department of Chemistry
Queen Mary's College University of Madras, Chennai – 600004, Tamil Nadu, India.

*Corresponding Author

Received on: 06-10-2017

Revised and Accepted on: 13-11-2017

DOI: <http://dx.doi.org/10.22376/ijpbs.2018.9.1.p1-15>



[Creative commons version 4.0](https://creativecommons.org/licenses/by-nc-sa/4.0/)

INTRODUCTION

Piperidine, morpholine and piperazine rings are structural units of many medicines which stimulate interest in the synthesis of novel derivatives of heterocyclic amines. Piperazine motif is a vital heterocyclic scaffold as constituent of numerous biologically active molecules. Piperazinyl linked Ciprofloxacin dimers are potent antibacterial, antimalarial and potential antipsychotic agents. Further, diphenylpiperazine derivatives possess extensive pharmacological action on central nervous system (CNS), especially on dopaminergic neurotransmission. Owing to the fascinating medicinal applications of these piperazine derivative synthesized drug discovery entities were shown good antimicrobial activity.¹⁻⁴ The application of this finding to our bridged piperazine, series has given us a group of β -branched Nitroolefin analogues. Nucleophilic addition of secondary

heterocyclic amines piperazine, tandem catalysis, hydroamino methylation and carbonylation etc., have been successfully synthesized and utilized for various organic transformations. Michael type addition of various kinds of nucleophiles to nitroolefins is one of the versatile synthetic methods in Organic chemistry leading to a C–C bond formation between a carbonyl compound and a nitro alkane.⁵⁻¹¹ Thus in this study piperazine derivatives were synthesized by Michael type addition and Baylis-Hilman adducts, further this derivative were subjected to antibacterial and for computational studies. Antibacterial activity was studied by MIC against the Gram positive and Gram negative organism for the synthesized compounds. Insilico docking studies have been carried out against the antibacterial protein Methionyl-tRNASynthetase4QRE using Discovery Studio 4.0. Further the pharmacokinetics properties were studied by ADMET. DMol³ Properties and B3LYP functions were also studied.

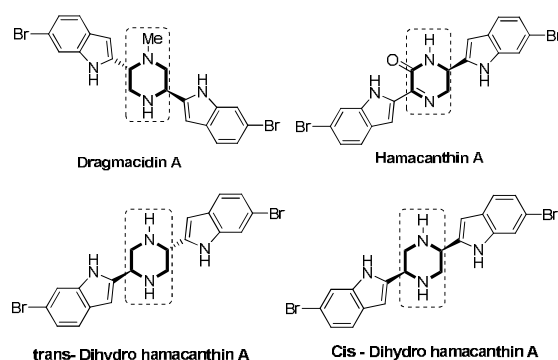


Figure 1

Selected example of Some of the analogous bio active molecules and natural Products embodying *N,N'*-disubstituted Piperazine Moiety and other Privileged motifs are shown below.

MATERIALS AND METHODS

Experiment

Melting points were recorded on a Super fit (India) capillary melting point apparatus and were uncorrected. For compounds ¹H NMR (300 MHz, CDCl₃) and ¹³C NMR (75 MHz, CDCl₃) spectra were recorded in deuterium chloroform (CDCl₃) on a Bruker 300 MHz spectrometer using tetramethylsilane (TMS, $\delta = 0$) as an internal standard at room temperature.

Synthesis of *N,N'*-disubstituted β -branched Nitroolefin Piperazines

A mixture of piperazine 1g of 1 equiv (11.609mmol) and 2 equiv of (23.20 mmol)(E)-(3-bromo-2-nitroprop-1-en-1-yl) benzene derivatives were added in 100 ml RB flask. 3 equiv of K₂CO₃ base in 30 ml of acetonitrile was added and then vigorously stirred in room temperature for 2hrs. The reactor was monitored by TLC analysis. After the completion of reaction, the crude mass was allowed to be purified by various fractions in column chromatography techniques using the mixture of 10% of Hexane: EtOAc as eluent. The spectrum characterization of 10a and 10k compounds were discussed in experimental section.

Antibacterial Investigations

A series of novel *N,N'*-disubstituted β -branched nitroolefin piperazine derivatives (10a–10k) were synthesized and their antimicrobial activity was evaluated by *in vitro* disc diffusion method and MIC by micro dilution method against standard strain of Gram-positive (+ve bacteria) *Staphylococcus aureus* (Sa), *Bacillus subtilis* (Bs), Gram (-ve bacteria) *Pseudomonas aeruginosa* (Pa), *Escherichia coli* (Ec), *Proteus mirabilis* (Pm) bacteria. The standard drug ciprofloxacin was used and (MIC) Minimum Inhibitory Concentration was estimated from 64 to 0.0625 μ g/ml concentrations.

Preparation of stock solution

Stock solutions of standard compound and synthesized compound of concentration 250 μ g/ml were prepared by dissolving 25mg of synthesized compound in 2ml of DMSO and made up to the volume 100 ml with sterile distilled water. From this stock solution different concentrations such as 64 μ g/ml, 32 μ g/ml, 16 μ g/ml, 8 μ g/ml, 4 μ g/ml, 2 μ g/ml, 1 μ g/ml, 0.5 μ g/ml, 0.25 μ g/ml, 0.125 μ g/ml were prepared.

Disc – diffusion method

The determination of the antibacterial activity of the compounds was performed by disc-diffusion method.¹³ Mueller Hinton agar was prepared according to the instructions of the manufacturer. All agar plates were prepared in 90 mm Petri dishes and 100 μ L of a suspension of the microorganisms was spread on solid media plates. Sterile filter paper discs (6 mm in diameter) were impregnated with 50 μ L of the sample solution in DMSO and placed on inoculated plates. After standing at 4°C for 2 h, the plates were incubated at 37°C for 24 h. Standard discs of ciprofloxacin were utilized as a positive control, while discs impregnated with 50 μ L of pure DMSO were utilized as a negative control. The diameters of the inhibition zones (including the disc) were calculated in milli meters. Each test was performed in triplicate.

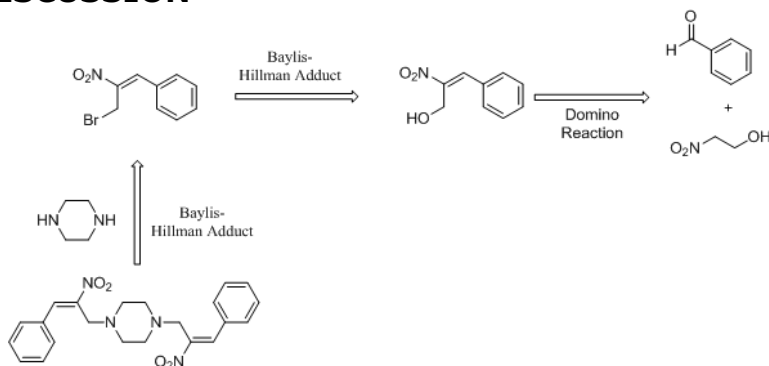
Determination of the Minimum Inhibitory Concentration (MIC)

The resolve of the minimum inhibitory concentration (MIC) was achieved by the broth micro dilution process in 96-well micro titer plates.¹² Sterile 96-well polystyrene microtiter plates with well capacities of 300 μ l were utilized and 100 μ l of fresh Mueller-Hinton broth was added to each well of the plate. One hundred μ L of the stock solution of the tested compounds in DMSO (concentration about 2 mg/100 μ L) was added to the wells of the first column. Then 100 μ l of the solution were eliminated from the first column and mixed thoroughly with the broth in the corresponding wells of the second column six times. Subsequently, a 100 μ L aliquot was eliminated from each well in this column and mixed with the broth in the corresponding well of the subsequently column. This doubling dilution was performed in rows across the plate. The similar procedure was repeated with stock solutions of each of the tested compounds. In the last row, double dilution was achieved with pure DMSO solution and this row was used as control. Ten μ L of the bacteria cultures was inoculated into each well of rows of the plate. The microtiter plate was incubated at 37°C for 24 h, after which the bacterial development was measured. The MIC was resolute as the lowest concentration that

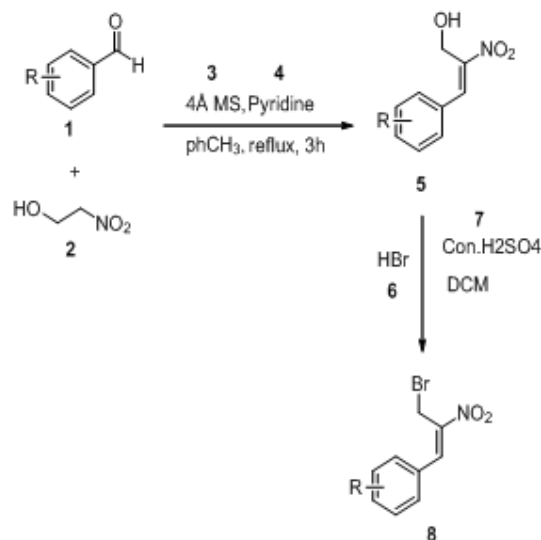
resulted in inhibition of bacterial development. Tests were accomplished in triplicate.

Molecular Docking, ADMET and DFT

The degree to which the synthesized novel Piperazine molecules will affect their target in conditions of structural and chemical complementation was investigated via the Flexible Docking module of the Discovery Studio 4.0. Molecular modeling interface.¹⁴⁻¹⁵ The binding energy will be calculated in D.S.4.0 and the following equation is $\text{Energy}_{\text{Binding}} = \text{Energy}_{\text{Complex}} - \text{Energy}_{\text{Ligand}} - \text{Energy}_{\text{Receptor}}$. Previous to docking, the protein 4QRE (Methionyl – tRNASynthetase) was prepared using the protein preparation wizard, eliminating the water molecule and cofactors from the proteins, optimizing hydrogen bonding and deleting the ligand present in the crystal structure.¹⁶⁻¹⁷ The selected 4QRE protein, selected (A-Chain) active site analysis discloses the 18 amino acids in the ligand binding pocket A:PRO11 A:ILE12 A:TYR14 A:ASP51 A:HIS53 A:GLY54 A:THR133 A:TYR134 A:PHE220 A:VAL234 A:TYR235 A:VAL236 A:TRP237 A:ASP239 A:ASN243 A:TYR244 A:ILE273 A:PHE276. All the molecules were docked into the active site of a target molecule, and ending scoring was carried out in terms of the Flexible Docking Version 4.0 function with high binding energy interaction between ligand – receptor cavity method. The drug likeness of the selected active *N, N'*-disubstituted β branched Nitroolefin Piperazine derivatives 10a-10k were investigated using Lipinski's and Veber rules. The properties are molecular weight < 500 Daltons, number of hydrogen bond donors < 5 and the number of hydrogen bond acceptors < 10. The ligands passing the Lipinski properties were taken for docking studies. As discussed by Lipinski, molecular properties are intimately related to the oral bioavailability of a drug. The D.S.4.0 was used to investigate drug likeness (Lipinski's Rule of Five), and (DFT) Density functional theory calculations using B3LYP functions, program (Discovery Studio DMol3 Version 4.0). The input parameter was preferred from D.S.4.0, DFT and DMol3 properties of total energy, binding energy, (HOMO) energy, (LUMO) energy, dipole Magnetic, (ESP) charge, band gap energy, dipole compound, Mulliken charge were estimated.

RESULTS AND DISCUSSION**Scheme 1**

Retrosynthetic approach for the synthesis of novel *N, N'*-disubstituted β -branched Nitroolefin Piperazines



Scheme 2
Synthesis of precursors 8

Table 1
Synthesis of *N, N'*-disubstituted β -branched Nitroolefin Piperazine frameworks (10a-10k).



Entry	R	Substrate	Product	Yield(%)
10a	H	9	10a	75
10b	2-me	9	10b	78
10c	4-me	9	10c	77
10d	4-et	9	10d	79
10e	2-OMe	9	10e	81
10f	4-OMe	9	10f	80
10g	3,4-OMe	9	10g	85
10h	2-Cl	9	10h	86
10i	Naphthalene	9	10i	88
10j	Furan	9	10j	91
10k	Thiophen	9	10k	90

1,4-bis((*E*)-2-nitro-3-phenylallyl)piperazine (10a)

Yield: 75%; Colour: white solid mp: 110 - 113°C; ¹H NMR (300MHz, CDCl₃): δ 2.52 (s, 4H), 3.68 (s, 2H), 7.25-7.65 (m, 5H), 8.16 (s, 1H); ¹³C NMR (CDCl₃, 75 MHz): 52.48, 52.37, 128.92, 130.54, 130.75, 132.03, 137.38, 148.84. Elemental Analysis for C₂₂H₂₄N₄O₄: Calculated: C, 64.69; H, 5.92; N, 13.67, O, 15.67; Found: 64.69; H, 5.92; N, 13.67, O, 15.67.

1,4-bis((*E*)-2-nitro-3-*o*-tolylallyl)piperazine (10b)

Yield: 78%; Colour: yellow solid mp: 115-118 °C; ¹H NMR (300MHz, CDCl₃): δ 2.33 (s, 3H), 2.418 (s, 4H), 3.58 (s, 2H), 7.26-7.49 (m, 4H), 8.18 (s, 1H); ¹³C NMR (CDCl₃, 75 MHz): δ 20.11, 52.12, 95.10, 126.28, 129.32, 130.25, 130.28, 130.30, 130.55, 130.87, 137.70. Elemental Analysis for C₂₄H₂₈N₄O₄: Calculated: C 66.04; H, 6.47;

N, 12.84, O, 14.66; Found: C 66.04; H, 6.47; N, 12.84; O, 14.66.

1,4-bis((*E*)-2-nitro-3-*p*-tolylallyl)piperazine (10c)

Yield: 77%; Colour: yellow solid mp: 116-119 °C; ¹H NMR (300MHz, CDCl₃): δ 2.41 (s, 3H), 2.54 (s, 4H), 3.70 (s, 2H), 7.25-7.27 (m, 2H), 7.56-7.59 (m, 2H), 8.18 (s, 1H); ¹³C NMR (CDCl₃, 75 MHz): δ 20.12, 52.12, 126.28, 129.34, 130.29, 130.55, 130.85, 137.71. Elemental Analysis for C₂₄H₂₈N₄O₄: Calculated: C 66.04; H, 6.47; N, 12.84; O, 14.66; Found: C 66.04; H, 6.47; N, 12.84; O, 14.66.

1,4-bis((*E*)-3-(4-ethylphenyl)-2-nitroallyl)piperazine (10d)

Yield: 79%; Colour: light brown solid; mp: 120-123 °C; ¹H NMR (300MHz, CDCl₃): δ 1.27 (t, *J* = 7.5 Hz, 3H), 2.56

(s, 4H), 2.71 (q, $J = 7.5$ Hz, 2H), 3.71 (s, 2H), 7.26-7.63 (m, 4H), 8.19 (s, 1H); ^{13}C NMR (CDCl_3 , 75 MHz): δ 15.21, 28.84, 52.39, 52.59, 128.57, 129.35, 131.18, 138.03, 147.61, 147.70. Elemental Analysis for $\text{C}_{26}\text{H}_{32}\text{N}_4\text{O}_4$: Calculated: C 67.22; H, 6.94; N, 12.06; O, 13.78; Found: C, 67.22; H, 6.94; N, 12.06; O, 13.78.

1,4-bis((E)-3-(2-methoxyphenyl)-2-nitroallyl) piperazine (10e)

Yield: 81%; Colour: yellow solid; mp: 131-134°C; ^1H NMR (300 MHz, CDCl_3): δ 2.48 (s, 3H), 3.63 (s, 2H), 3.87 (s, 4H), 6.91-7.78 (m, 4H), 8.40 (s, 1H); ^{13}C NMR (CDCl_3 , 75 MHz): δ 52.45, 52.76, 55.60, 110.60, 120.65, 121.20, 131.33, 132.15, 132.23, 148.43, 158.32. Elemental Analysis for $\text{C}_{24}\text{H}_{28}\text{N}_4\text{O}_4$: Calculated: C 6.53; H, 6.02; N, 11.96; O, 20.49; Found: C 6.53; H, 6.02; N, 11.96; O, 20.49.

1,4-bis((E)-3-(3-methoxyphenyl)-2-nitroallyl) piperazine (10f)

Yield: 80%; Colour: yellow solid; mp: 135-138 °C; ^1H NMR (300 MHz, CDCl_3): δ 2.60 (s, 4H), 3.73 (s, 2H), 3.88 (s, 3H), 6.98 (d, $J = 6.0$ Hz, 2H), 7.72 (d, $J = 8.7$ Hz, 2H), 8.24 (s, 1H); ^{13}C NMR (75 MHz, CDCl_3): δ 52.32, 52.68, 55.48, 114.56, 124.46, 133.46, 138.48, 148.08, 161.92. Elemental Analysis for $\text{C}_{24}\text{H}_{28}\text{N}_4\text{O}_4$: Calculated: C 61.53; H, 6.02; N, 11.96; O, 20.49; Found: C 61.53; H, 6.02; N, 11.96; O, 20.49.

1,4-bis((E)-3-(3,4-dimethoxyphenyl)-2-nitroallyl) piperazine (10g)

Yield: 85 %; Colour: yellow solid; mp: 136-139°C; ^1H NMR (300 MHz, CDCl_3): δ 2.61 (s, 4H), 3.74 (s, 2H), 3.94-3.96 (d, $J = 6.9$ Hz, 6H), 6.95 (d, $J = 8.4$ Hz, 1H), 7.34 (d, $J = 8.1$ Hz, 1H), 7.59 (s, 1H), 8.28 (s, 1H); ^{13}C NMR (CDCl_3 , 75 MHz): δ 52.49, 52.95, 56.04, 111.12, 113.70, 124.88, 126.31, 139.34, 145.84, 149.24, 151.73. Elemental Analysis for $\text{C}_{26}\text{H}_{32}\text{N}_4\text{O}_8$: Calculated: C 59.08; H, 6.10; N, 10.60; O, 24.22; Found: C 59.08; H, 6.10; N, 10.60; O, 24.22.

1,4-bis((E)-3-(2-chlorophenyl)-2-nitroallyl) piperazine (10h)

Yield: 86 %; Colour: brown solid; mp: 125-128°C; ^1H NMR (300 MHz, CDCl_3): δ 2.40 (s, 4H), 3.56 (s, 2H), 7.32-7.66 (m, 4H), 8.21 (s, 1H); ^{13}C NMR (CDCl_3 , 75 MHz): δ 52.41, 52.60, 126.93, 129.85, 130.78, 131.12, 131.21, 133.45, 134.79, 150.25. Elemental Analysis for $\text{C}_{22}\text{H}_{22}\text{ClN}_4\text{O}_4$: Calculated: C 55.36; H, 4.65; Cl, 14.85; N, 11.74; O, 13.41; Found: C 55.36; H, 4.65; Cl, 14.85; N, 11.74; O, 13.41.

1,4-bis((E)-3-(naphthalen-1-yl)-2-nitroallyl) piperazine (10i)

Yield: 88%; Colour: white solid; mp: 140-144°C; ^1H NMR (300 MHz, CDCl_3): δ 2.31 (s, 4H), 3.54 (s, 2H), 7.45-7.92 (m, 7H), 8.58 (s, 1H); ^{13}C NMR (CDCl_3 , 75 MHz): δ 52.53, 52.76, 123.96, 125.19, 11.02; O, 12.58 126.62, 127.25, 128.00, 128.87, 128.93, 130.56, 131.51, 133.37, 134.35, 150.49. Elemental Analysis for $\text{C}_{30}\text{H}_{28}\text{N}_4\text{O}_4$: Calculated: C 70.85; H, 5.55; N, 11.02; O, 12.58; Found: C 70.85; H, 5.55; N, 11.02; O, 12.58.

1,4-bis((E)-3-(furan-3-yl)-2-nitroallyl) piperazine (10 j)

Yield: 91%; Colour: Light yellow; mp: 108-112°C; ^1H

NMR (300 MHz, CDCl_3): δ 2.56 (s, 4H), 3.95 (s, 2H), 6.56-7.63 (m, 3H), 7.89 (s, 1H); ^{13}C NMR (CDCl_3 , 75 MHz): δ 52.76, 113.03, 120.72, 123.04, 144.83, 146.60, 147.36. Elemental Analysis for $\text{C}_{18}\text{H}_{20}\text{N}_4\text{O}_6$: Calculated: C 55.67; H, 5.19; N, 14.43; O, 24.72; Found: C 55.67; H, 5.19; N, 14.43; O, 24.72.

1,4-bis((E)-2-nitro-3-(thiophen-3-yl)allyl) piperazine (10k)

Yield: 90%; Colour: light green; mp: 110-113°C; ^1H NMR (300 MHz, CDCl_3): δ 2.59 (s, 4H), 3.82 (d, $J = 3.6$ Hz, 2H), 7.16-7.71 (m, 3H), 8.41 (d, $J = 3.6$ Hz, 1H); ^{13}C NMR (CDCl_3 , 75 MHz): δ 52.44, 52.94, 128.03, 130.84, 134.01, 134.36, 136.41, 145.14. Elemental Analysis for $\text{C}_{18}\text{H}_{20}\text{N}_4\text{O}_4\text{S}_2$: Calculated: C 51.41; H, 4.79; N, 13.32; O, 15.22; S, 15.25; Found: C 51.41; H, 4.79; N, 13.32; O, 15.22; S, 15.25. The Baylis–Hillman (BH) reaction is significant carbon–carbon bond forming reaction which has seen enormous development in recent years. It is fine documented that Baylis–Hillman adducts have been utilized in the synthesis of a spacious diverse of natural products and medicinally active components. An original protocol for the capable construction of *N, N'*-disubstituted β -Branched Nitroolefin Piperazines was reported as the outcome of the unending research interest of the authors in heterocyclic chemistry. Owing to the biological importance of Piperazine, It was visualized that the synthesis of *N, N'*-disubstituted β -Branched Nitroolefin Piperazine is a promising source to achieve a lot of Pharmacological significant therapeutic applicable strategy. To synthesis the key initial material for the execution of our goals, we have prepared (E)-2-nitroallylic alcohol **5** from the reaction of substituted aromatic aldehyde **1**, 2-Nitroethanol **2**, 4Å MS (Molecular sieves) **3**, pyridine **4**, giving only the desired starting material derivative of **5**, by performing the reaction on **3** activated 4Å Molecular Sieves are conditions absolutely required to obtained entire alteration and whole intermediate dehydration beyond by these results, pyridine used as a catalyst of these effortless and capable synthesis protocol, the Toluene used as a solvent. Here, the domino reaction progress with high stereo selectivity one-pot method. They also synthesized antifungal agent utilizing the bromo derivative of a Baylis–Hillman adduct as a starting material **5a** lot of reports are offered in the literature signifying the synthetic utility of bromo derivatives of Baylis–Hillman adducts in the synthesis.⁷ Based on these reports, we predicted that the bromo compounds derived from nitroolefins will also supply as admirable building blocks for the synthesis of a spacious diversity of useful compounds. Triggered by this idea, we decided to prepare the bromo compound derived from nitroolefins, which will yield new novel *N, N'*-disubstituted β -branched Nitroolefin Piperazine derivatives of the Baylis–Hillman adducts with (E)-(3-bromo-2-nitroprop-1-en-1-yl)benzene derivatives of (**8a** – **8k**) and piperazine **9** under the influence of K_2CO_3 in acetonitrile lead to the required precursor **8**. (Scheme 2), which will be extremely valuable in synthesizing the potent enormous biological activity of *N, N'*-disubstituted β -branched Nitroolefin Piperazine frameworks according to the retro-synthetic way shown in Scheme 1. The desired *N, N'*-disubstituted β -branched Nitroolefin Piperazine derivatives shown in (Table 1) entry (10a-

10k). Totally eleven novel therapeutic Application for *N,N'*-disubstituted β -Branched Nitroolefin Piperazine derivatives were synthesized. The recorded NMR

spectra of ^{13}C and ^1H compound 10g using chloroform (CDCl_3) and 300MHZ are depicted in Figure 2 and Figure 3.

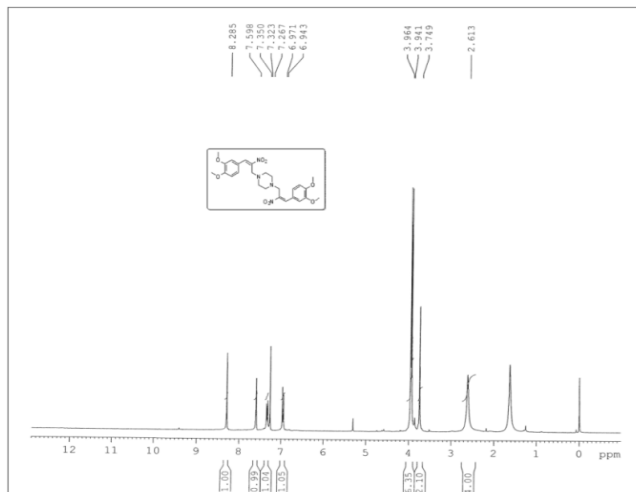


Figure 2
 ^1H Spectrum of Compound in CDCl_3 Solvent (10g).

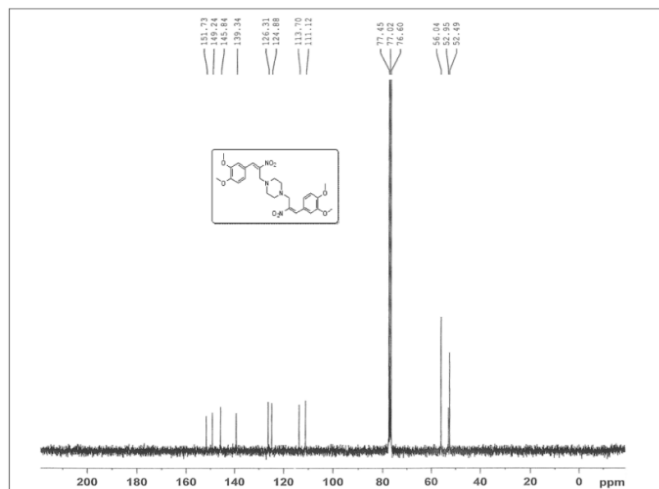


Figure 3
 ^{13}C Spectrum of Compound in CDCl_3 Solvent (10g).

^{13}C and ^1H NMR Spectral analysis

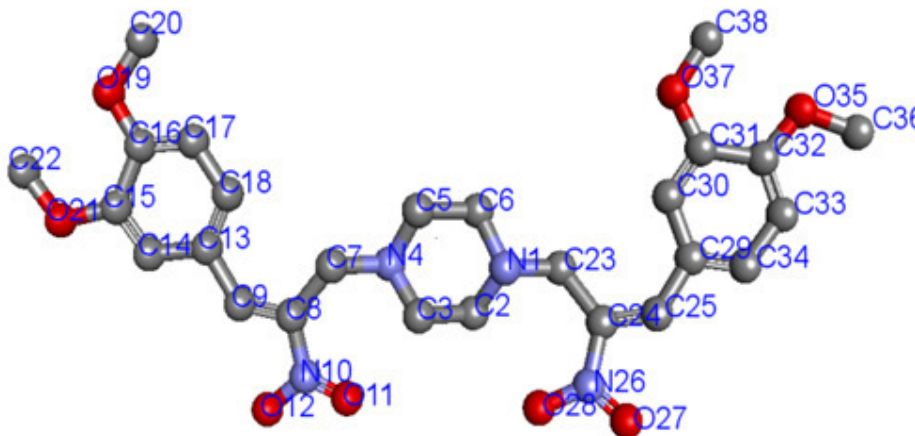


Figure 4
2D structure of Piperazin Derivative 10g

^1H NMR (300 MHz, CDCl_3): δ 2.61 (s, CH_2 , 4H), 3.74 (s, CH_2 , 2H), 3.94-3.96 (d, $J = 6.9$ Hz, O - CH_3 , 6H), 6.95 (d, $J = 8.4$ Hz, Ar-H, 1H), 7.34 (d, $J = 8.1$ Hz, Ar-H, 1H), 7.59 (s, Ar-H, 1H), 8.28 (s, (C=C)1H); ^{13}C NMR (CDCl_3 , 75 MHz): δ 52.49, 52.95, 56.04, 111.12, 113.70, 124.88, 126.31, 139.34, 145.84, 149.24, 151.73.

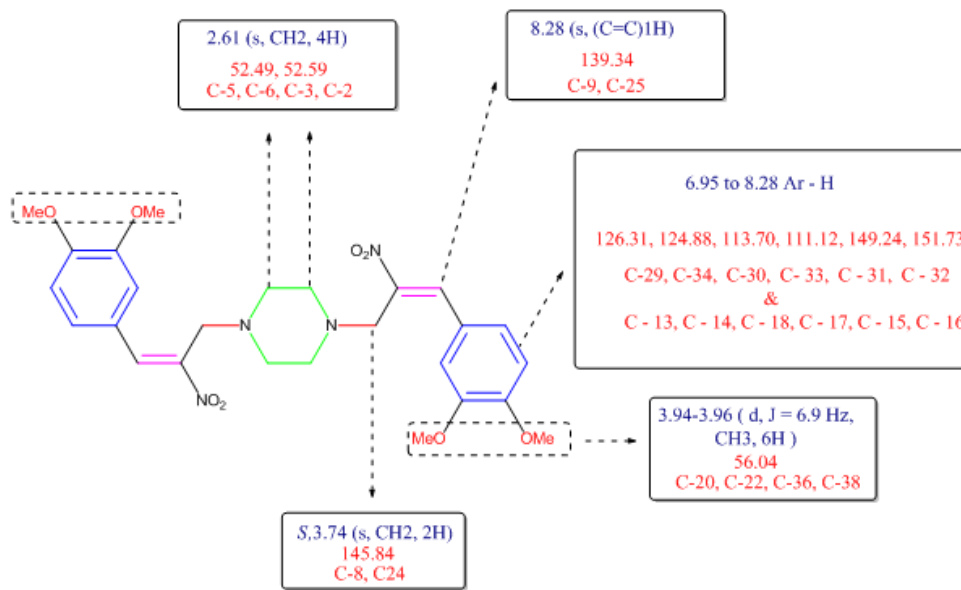


Figure 5
Key NMR data of compound 10g

The ^1H NMR and ^{13}C NMR spectrum of 10g demonstrated a singlet at δ 2.61 ppm due to the methylene protons of piperazine ring, which shows with C- 5, C- 6, C- 3 and C- 2 Carbon at δ 52.49 ppm and 52.95 ppm. The signal 3.74 ppm has 2 proton methylene carbon, respectively, Unambiguous assignment of carbon C - 8, C - 14 of 10g to the signal of δ 145.84 ppm (Figure 5). From C, H-correlations, the doublet at δ 3.94 and 3.96 ppm were assigned to O- CH_3 protons. The methyl proton (CH_3) appeared as triplet at δ 56.04 ppm, Unambiguous assignment of carbon C-20, C-22, C-36 and C-38. The signal at C-9 and C-25, respectively at δ 139.34 ppm (C=C ethylene) Carbon and its proton NMR signal was shown at δ 8.28 ppm. The aromatic protons appear as multiplets in the range δ 6.95 to 8.28 ppm proton, respectively unambiguous assignment of carbon C-29, C-34, C-30, C-33, C-31, C-32 and C-13, C-14, C-18, C-17, C-15, C-16. The doublet proton of 3.94 and 3.96 ppm of O- CH_3 group was present in 10g 1,4-bis((E)-3-(3,4-dimethoxyphenyl)-2-nitroallyl)piperazine compound, recently O-methoxy group was proved highly biological activity in many research work. Benzyl piperazine analogues (10g) showed potent activity against Gram positive and significant activity against Gram negative bacterial strains. Compound 10g having benzyl group in piperazine and methoxy group in phenacyl nucleus in ^1H NMR signal δ 3.94-3.96 (d, $J = 6.9$ Hz, O - CH_3 , 6H) and ^{13}C NMR signal at C-20, C-22, C-36 and C-38, respectively at δ 56.04 ppm was shown in (Figure 5). Hence, the compound 10g exhibited potent activity against Gram-positive (+ve bacteria) *Staphylococcus aureus* (Sa) (MIC = 0.125 $\mu\text{g/ml}$), *Bacillus subtilis* (Bs) (MIC = 0.5 $\mu\text{g/ml}$), Gram (-ve bacteria), *Pseudomonas aeruginosa* (Pa) (MIC = 2 $\mu\text{g/ml}$), *Escherichia coli* (Ec) (MIC = 0.5 $\mu\text{g/ml}$), *Proteus*

mirabilis (Pm) (MIC = 0.5 $\mu\text{g/ml}$). Since this compound has a promising source of high biological activity of (MIC) antibacterial studies and disc diffusion method shown in (Table 3 and Figure 8) and also showed high antibacterial activity in disc diffusion method in (Table 2, Figure 6 and Figure 7). Further *in-silico* studies the compound 10g exhibit granted good results while compared to other compounds.

Antibacterial activity by disc diffusion method

The antibacterial activities of 10g, 10j and piperazine derivatives of novel *N, N'*-disubstituted β -branched nitroolefins were first tested by the agar disc diffusion method against Gram-positive and Gram-negative bacteria. The results of these studies, signified as zones of inhibition, are summarized in (Table 2, Figure 6 and Figure 7). As can be seen from the data, both 10g and 10j expressed activity against all investigated bacteria cells. It was assumed that 10g of aryl-piperazine would reveal antibacterial activity. It was found that the majority of the synthesized derivatives displayed *in vitro* antibacterial activity against selected bacteria. Some derivatives confirmed a superior activity than the preparatory compounds. These results specified a potential synergistic antibacterial upshot of synthesized derivatives Compared with compound 10a, introduction of innovative groups in the aromatic moiety of 10g in a little cases granted derivatives with a superior antibacterial activity. Since the outer layer of Gram-negative bacteria is negatively charged, it was expected, that the majority of the 10g 3,4-OMe derivative of *N, N'*-disubstituted piperazine with delocalized positive charge at the o-methoxy moiety, would confirm a superior activity toward Gram-negative bacteria, which was indeed observed, excluding in the case of *Proteus mirabilis*. The derivative 10j and 10d possessed a

moderate activity while derivatives 10b and 10k did not show superior antibacterial activity. It seems that introduction of a substituent at position 2-me and thiophene afforded derivatives with not better antibacterial activity. Derivative 10h confirmed momentous activity towards the majority of the selected bacterial strains. Against the selected Gram-positive bacteria, the derivatives 10c, 10i and 10j were highly active. As with the Gram-negative bacteria, derivative

10d, 10g and 10h expressed excellent activity. Derivatives 10e and 10k did not exhibit better antibacterial activity. Other derivatives displayed a moderate activity against all chosen bacteria cells. It was pragmatic that, as in the cases of the Gram-negative bacteria, the most active were those derivatives that have a substituent with a positive resonance effect on the aromatic ring.

Table 2
In vitro antibacterial activity (mm) against Gram-positive and Gram –negative bacteria at a concentration of 64µg/disc.

S.No.	Compound Name	Zone of Inhibition in (mm)	
		64µg/disc	
		Salmonella typhi	Proteus mirabilis
1	10a	7	8
2	10b	7	7
3	10c	8	7
4	10d	5	10
5	10e	6	6
6	10f	7	7
7	10g	7	10
8	10h	7	9
9	10i	8	7
10	10j	9	7
11	10k	6	6
12	Ciprofloxacin	26	23

Inactive Concentration 30 µg/disc. DMSO Solvent: Positive control: Ciprofloxacin.

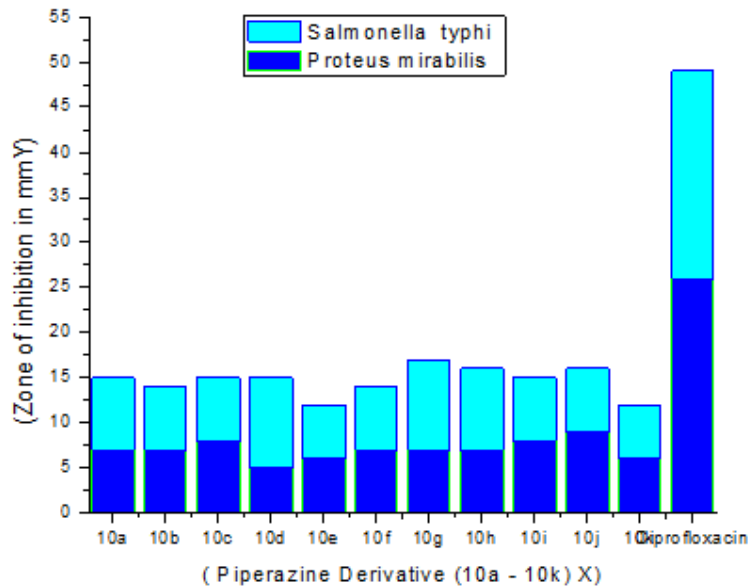


Figure 6
In vitro antibacterial activity of disc-diffusion method of Graphical representation for Piperazine derivatives (10a–10k).

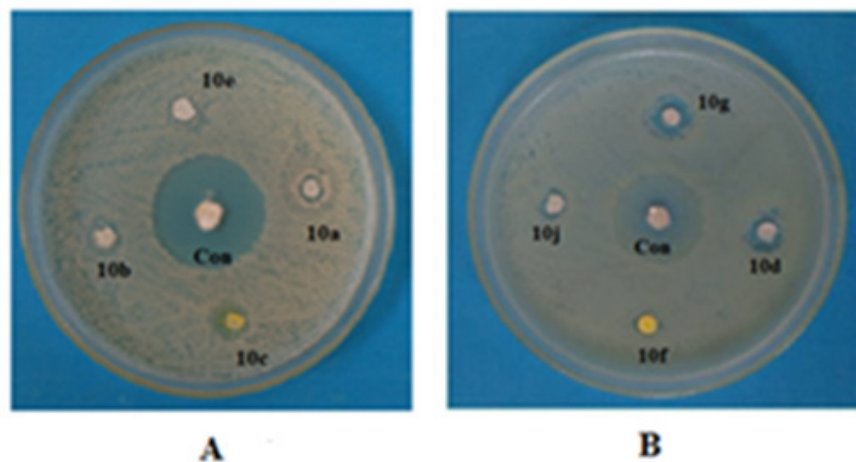


Figure 7
Antibacterial activity (A and B) Disc plate image
of Piperazine derivative (10a-10k).

Antibacterial activity by (MIC) method

N, N'-disubstituted β -branched Nitroolefin Piperazine derivatives (10a-10k) were synthesized and screened for their efficiency as antimicrobials against diverse pathogens *in vitro* by broth micro dilution process. Ciprofloxacin was utilized as a standard against both Gram-positive and Gram-negative bacteria. The results are shown in (Table3) and Graphical representation of Piperazine derivatives (10a-10k) are shown in (Figure 8). Piperazine analogues are known to have antibacterial activity.¹⁸⁻¹⁹ The (E)-(3-bromo-2-nitroprop-1-en-1-yl)benzene Derivatives (8a – 8k) and (9) attached 1,4-disubstituted piperazine granted organic synthesis technique product of (10a-10k) which used to improving antibacterial activity of piperazine class of molecules which have nitro alkenes their significant as biological and pharmacological active substance. The piperazine series (10a-10k), compounds 10c, 10d, 10e, 10h, 10i, 10a, 10b and 10g showed significant MIC activity in the order 10g > 10c, 10d, 10j > 10e, 10f, 10k > 10h > 10i > 10a > 10b against both Gram – positive and Gram – negative bacteria in MICs ($\mu\text{g/ml}$) which shown in (Table 2 and Figure 2) All the *N, N'*-disubstituted β -branched Nitroolefin Piperazine derivatives (10a-10k) 2-

NO_2 located in C8 and C17 Carbon, showed superior activity in this series, compound 10g having a nitro group and the position 3,4- OMe group showed good activity than other compounds in the series (10a-10k). The range of MIC values for this derivative was 0.125 – 0.5 $\mu\text{g/ml}$. Introducing the derivative of 4-me group in 10c, 4-et group in 10d and furan group 10j demonstrates better activity against both gram-positive and gram-negative bacteria. The derivatives of 10e 2-Ome, 10f 4-Ome and 10k thiourea groups generate enhanced activity against gram positive than gram negative bacteria. As the electron negativity increases, the inhibition also increases as we observed from the derivative 2-Chloro group in 10h. Similarly in the presence of Naphthalene group 10i demonstrates higher activity against gram – positive *Staphylococcus aureus* (Sa) bacteria which has the MIC value of 0.5 $\mu\text{g/ml}$. 10a showed modest activity where as in the presence of phenyl- H group. This highlights that, the nature of the functional linkage (NO_2 , OMe, Cl, and *N, N'*-disubstituted piperazine) influences the antibacterial activity. Ultimately, the above four structural correlation studies expose that both nucleus and substituents are liable for the antibacterial activity.

Table 3
MIC ($\mu\text{g/ml}$) value of *N, N'*-disubstituted β -branched Nitroolefin Piperazine derivatives (10a-10k)
against gram (+ ve bacteria) & gram (- ve bacteria)
in DMSO solvent

S.No.	Sa	Bs	Pa	Ec	Pm
10a	2	4	8	4	4
10b	4	8	8	8	8
10c	0.25	2	4	2	2
10d	0.25	2	4	2	2
10e	2	2	4	2	2
10f	2	2	4	2	2
10g	0.125	0.5	2	0.5	0.5
10h	0.5	2	8	2	2
10i	0.5	4	8	2	4
10j	0.25	2	4	2	2
10k	2	2	4	2	2
Ciprofloxacin	0.25	0.5	0.12	0.063	0.125

Staphylococcus aureus (Sa), *Bacillus subtilis* (Bs), *Pseudomonas aeruginosa* (Pa), *Escherichia coli* (Ec), *Proteus mirabilis* (PM).— Indicates bacteria are resistant to the compounds 0.0625 to 64 $\mu\text{g/ml}$. MIC ($\mu\text{g/ml}$) = minimum inhibitory concentration, that is lowest concentration to completely inhibit bacterial growth.

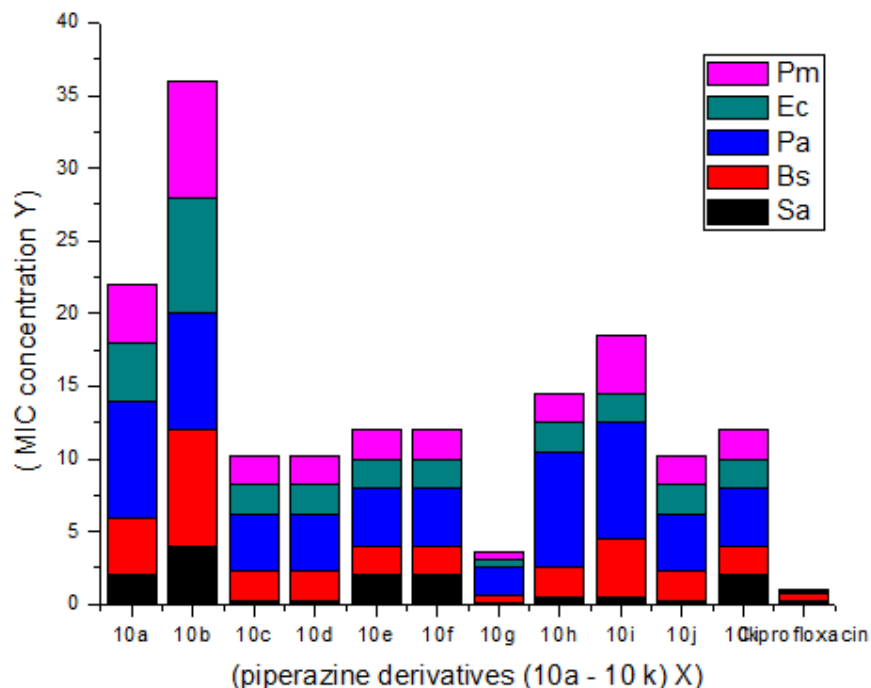


Figure 8

(MIC) Antibacterial activity of Graphical representation for Piperazine derivatives (10a–10k). *Staphylococcus aureus* (Sa), *Bacillus subtilis* (Bs), *Pseudomonas aeruginosa* (Pa), *Escherichia coli* (Ec), *Proteus mirabilis* (PM).

In silico docking of Piperazine derivatives (10a-10k) for 4QRE protein inhibition

The Methionyl-tRNA Synthetase 4QRE antibacterial protein was chosen as the target, X-ray diffraction resolution value is 1.7 Å, and the source of organism is *Staphylococcus aureus* (Sa). 265 poses were generated for Piperazine derivative (10a-10k) results in Flexible Docking D.SV4.0. [16]. The high results of Receptor – surface 10g Molecular Docking images was shown in (Figure 9). The 2D ligand-protein residues interaction scheme of 10g was shown in (Figure 10). The compound 10g 1,4-bis((E)-3-(3,4-dimethoxyphenyl)-2-

nitroallyl)piperazine shows higher “ligand –receptor” binding interaction of -162.782. The ligand interaction with the amino acids [LYS311]N-H...O with its bond angle of 2.91Å, [LYS311]N-H...O with its bond angle of 2.48Å, [LYZ311]N-H...O interaction with its bond angle of 2.04Å, C-H...O[GLU132] with its bond angle of 2.53Å, C-H...O[GLU132] with its bond angle of 2.86Å, C-H...O[GLU132] with its bond angle of 2.81Å were observed. Since the ligand 10g showed promising interaction and high binding energy against the 4QRE Pyrimidine Antibacterials Targeting Methionyl-tRNA Synthetase.

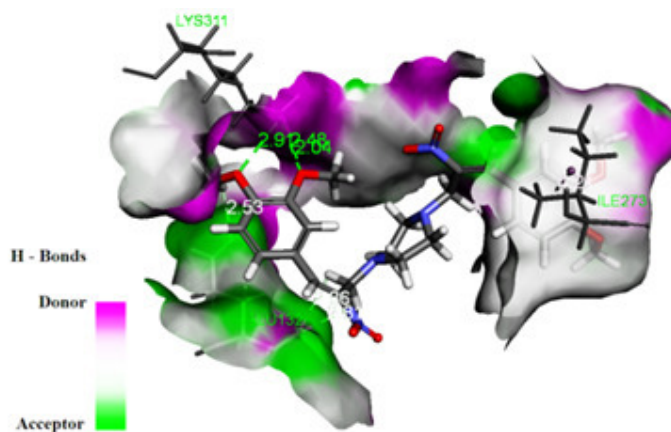


Figure 9

The docking pose of 10g 1,4-bis((E)-3-(3,4-dimethoxyphenyl)-2-nitroallyl)piperazine in the receptor site.

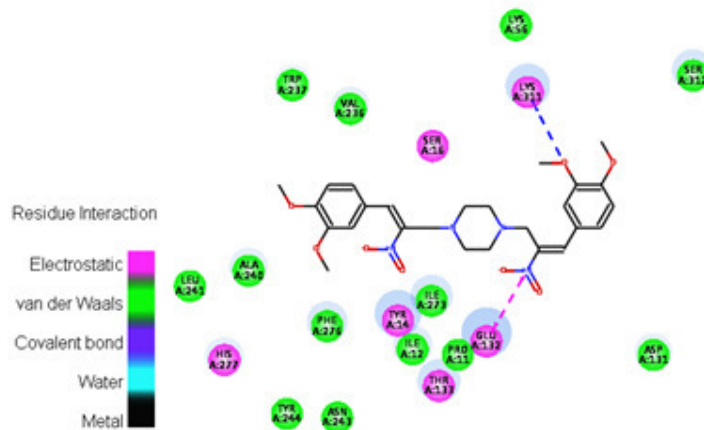


Figure 10

2D ligand – protein residues interaction scheme for 10g 1,4-bis((E)-3-(3,4-dimethoxyphenyl)-2-nitroallyl)piperazine.

ADMET (absorption, distribution, metabolism, excretion, and toxicity) analysis studies

We have analyzed diverse pharmacokinetic and pharmacodynamic properties of 11 new compounds recently designed *N, N'*-disubstituted β -branched nitroolefin piperazine analogs. The ADMET analysis was significant in drug design, a few properties together with human intestinal absorption (HIA), aqueous solubility level, BBB penetration levels, CYP2D6 inhibition of these 11 new compounds were analyzed. The ADMET plot is a 2D chart of ADMET_PSA_2D (Fast polar surface area) versus ADMET_AlogP98 (ALogP).²⁰ The

two sets of ellipses are for the prediction confidence space (95% and 99%) for the Blood Brain Barrier Penetration and Human Intestinal Absorption models, respectively. The pharmacokinetic results were shown in (Figure 11 and Table 4). The toxicity profile of the compounds were predicted utilizing TOPKAT which used a range of quantitative structure toxicity relationship (QSTR) models for assess in special toxicological endpoints such as aerobic biodegradability, mutagenicity, developmental toxicity prediction, skin irritation test. ADMET-TOX prediction results in lead optimization.²¹ showed in (Table 5).

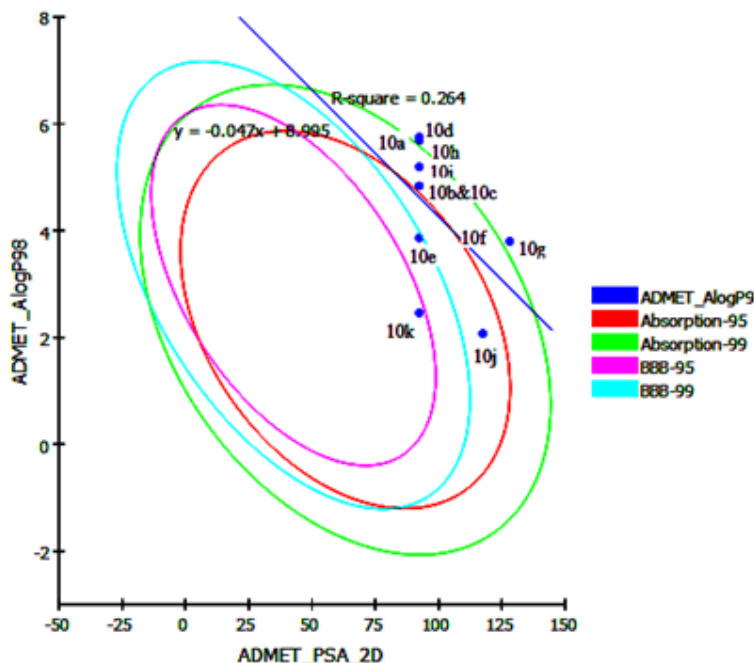


Figure 11

Graphical representation of ADMET properties of 10a-10k *N, N'*-disubstituted β -branched nitroolefin Compounds.

Table 4
ADMET Pharmacokinetic properties

Compound S.No	Solubility Level	BBB level	Absorbtion Level	CYP2D6	Hepatotoxic	PPB	AlogP98	PSA_2D
10a	2	2	0	-4.02034	-4.86006	4.47413	3.864	92.351
10b	2	4	1	-3.19217	-3.68856	5.25391	4.836	92.351
10c	2	4	1	-4.31611	-4.88554	5.52893	4.836	92.351
10d	2	4	2	-4.27014	-4.56434	4.15636	5.749	92.351
10e	2	4	1	-3.73221	-3.71474	2.33732	3.831	110.211
10f	2	4	1	-5.73896	-4.0576	4.00922	3.831	110.211
10g	3	4	2	-6.43219	-3.98585	3.53937	3.798	128.071
10h	2	4	1	-1.73713	-2.34842	6.47661	5.193	92.351
10i	3	3	0	-3.46334	-0.840304	0.965612	2.459	92.351
10j	3	4	0	-6.52275	-0.486858	0.645975	2.072	117.459
10k	1	4	2	-2.4621	1.35285	3.15817	5.681	92.351

An HIA level of 0 indicates a good absorption, its value of ADMET_Absorption_T2_2D < 6.1261 (inside 95%). The compounds 10a, 10i and 10j were predicted 0 in the level of HIA after oral administration. The drug likeness properties of ADMET aqueous solubility level log (Sw) must be more than 0.0, and should have moderate or good intestinal absorption. Aqueous solubility utilized to predict the solubility of compounds in water at 25°C and it has six assorted levels from 0-6. The synthesized compound of 10g, 10i and 10j were predicted in the level of 3, its value of (-4.0 <log (Sw) < -2.0) showed a good solubility range compared with other compound.

The blood-brain barrier (BBB) is a complex cellular system helps to maintain the homeostasis of the central nervous system (CNS) by separating the brain from the systemic blood circulation. Drugs have the possibility to cross the blood brain barrier. Compounds 10a was predicted in the level of 2, its value of (-0.52 <logBB< 0) showed a medium penetration to moderate cross the blood brain barrier. The hepatotoxic level for (10a-10j) compounds were predicted to be in the level of 0 based on Non-Toxic in ADMET results were shown in (Table – 4).

Table 5
Toxicity profile of (10a-10k) ligands using Toxicity prediction – Extensible protocol in Accelrys Discovery studio 4.0.

Ligand	AMES Mutagenicity	Developmental Toxicity Potential	Ocular Irritancy	Skin irritancy	Skin Sensitizer	Carcinogenicity			
						Female Mouse	Male Mouse	Female Rat	Male Rat
10a	Non-Mutagen	Toxic	None	None	Strong	Non-Carcinogen	Non-Carcinogen	Non-Carcinogen	Non-Carcinogen
10b	Non-Mutagen	Toxic	Severe	Mild	Strong	Non-Carcinogen	Non-Carcinogen	Carcinogen	Non-Carcinogen
10c	Non-Mutagen	Toxic	Severe	Mild	Weak	Non-Carcinogen	Non-Carcinogen	Carcinogen	Non-Carcinogen
10d	Non-Mutagen	Toxic	Severe	None	Strong	Non-Carcinogen	Non-Carcinogen	Non-Carcinogen	Non-Carcinogen
10e	Non-Mutagen	Toxic	None	None	Strong	Non-Carcinogen	Carcinogen	Non-Carcinogen	Carcinogen
10f	Non-Mutagen	Toxic	Mild	None	Strong	Non-Carcinogen	Non-Carcinogen	Non-Carcinogen	Non-Carcinogen
10g	Non-Mutagen	Toxic	Mild	None	Strong	Non-Carcinogen	Non-Carcinogen	Non-Carcinogen	Non-Carcinogen
10h	Non-Mutagen	Toxic	Mild	Mild	Strong	Non-Carcinogen	Non-Carcinogen	Non-Carcinogen	Non-Carcinogen
10i	Mutagen	Toxic	Mild	Mild	None	Carcinogen	Carcinogen	Non-Carcinogen	Carcinogen
10j	Non-Mutagen	Toxic	Severe	Mild	Weak	Non-Carcinogen	Carcinogen	Carcinogen	Carcinogen
10k	Non-Mutagen	Toxic	Severe	Mild	Strong	Non-Carcinogen	Carcinogen	Carcinogen	Carcinogen

In toxicity prediction – extensible bayesian models are used to predict the toxicity of synthesized derivative(10a – 10k) ligands by D.S.4.0.²² Toxicity profile includes screening for AMES Mutagenicity, developmental toxicity potential, ocular irritancy, skin irritancy, skin sensitizer and carcinogenicity were performed well.

All the compounds were non-mutagenic in AMES mutagenicity screening except 10i. While (DTP) Development Toxicity Potential of compounds (10a-10k) had shown Toxicity. The compound (10b, 10c, 10d, 10j and 10k) had shown severe ocular irritancy. The compounds (10b, 10c, 10h, 10i, 10j and 10k) showed mild skin irritancy, all the compounds had shown strong in skin sensitizers excluding 10c, 10i and 10j. The compound 10i were both carcinogenic in female and male mouse, and the compound 10i, 10j and 10k are carcinogenic in male mouse. All the compounds are non-carcinogen in female rat excluding 10b, 10c, 10j and 10k. The compound 10a, 10b, 10c, 10d, 10f, and 10g were shown in non-carcinogen. Finally the compound 10g were non-mutagen and non-carcinogen in nature.

Frontier molecular orbitals (FMOs) and DFT (Density Functional Theory) Studies

The Density Function Theory (DFT) was calculated by B3LYP exchange-correlation potential functional of Dmol3 in (Discovery Studio) D.S.4.0. It was utilized for calculating the orbital energies. Density functional theory begins with a theorem by Hohenberg and Kohn later generalized by Levy,²³ which states that all ground-state properties are functionals of the electron density ρ . Specifically, the total energy E_t may be written as in equation $E_t[\rho] = T[\rho] + U[\rho] + E_{xc}[\rho]$. where $T[\rho]$ is the kinetic energy of a system of non interacting particles of density ρ , $U[\rho]$ is the classical electrostatic energy due to coulombic interactions, and $E_{xc}[\rho]$ includes all many-

body contributions to the total energy, in particular the exchange and correlation energies. The energies of the HOMO and LUMO frontier orbitals are responsible for charge transfer in a chemical reaction. According to the frontier molecular orbital theory, HOMO and LUMO are the essentially momentous factors that affect the bioactivity. HOMO has the priority to provide electrons (electron donor), whereas LUMO can accept electrons (electron acceptor). The HOMO and LUMO characterize the susceptibility of the molecule to assault by electrophiles and nucleophiles, respectively. A high HOMO energy will be like matched up to a elevated activity of the compound. The gap between the LUMO and HOMO energies, called the band gap, illustrates the reactivity of a molecule. A broad gap disfavors the excitation of an electron from the HOMO to the LUMO, which consequently guides to a weaker affinity of the inhibitor to the target protein. Therefore, compounds with smaller band gaps are comparatively more reactive.²⁴⁻²⁵ The HOMO and LUMO respectively, π bonding and π^* anti-bonding orbitals upshot by cause of the sideways in phase and out of phase overlap of π atomic orbitals respectively. The enhance in bonding character of molecular orbital is reasoned by the hyper-conjugation effect and is reflected as great overlapping of molecular orbitals, since the electrons are spread over many orbitals. Thus, study of the frontier orbital

energy can grant useful information about the biological mechanism. It is evident from the (Figure 12) that, the HOMO levels are spread mainly over substituted 3,4-OMe phenyl ring to LUMO *N,N*-disubstituted β -branched nitroolefin piperazine ring. The calculated energy value of HOMO and LUMO are -0.169242 and -0.101904 (Kcal/mol) and the frontier orbital gap is 0.0673375 for a compound of 10g given in (Table 6). The isosurface of the electron density colored by the electrostatic potential molecules. By default, the isovalue of the electron density was 0.03, and the coloring scheme was spectrum Rainbow1 with a range from the default value -0.05 to 0.1 was shown in color. From the default value -0.05 to 0.1 was shown in color, the molecular electrostatic potential diagram shown in (Figure 13). Finally, the hit compound 10g that mapped well to the pharmacophoric features were characterized as final hits to the bioactive molecules. Typically, pharmacophore features include hydrophobic, aromatic, hydrogen bond acceptor, hydrogen bond donor, positive ionizable and negative ionizable. The pharmacophore model consists of one Hydrogen Bond Acceptor (HBA, in green), two Hydrophobic centers (in light blue). Two benzene substituted 3,4-OMe group presented in Ring_Aromatic Orange in colour, and the *N,N*-disubstituted benzene ring two Pos_ionizable was presented in (Figure 14).

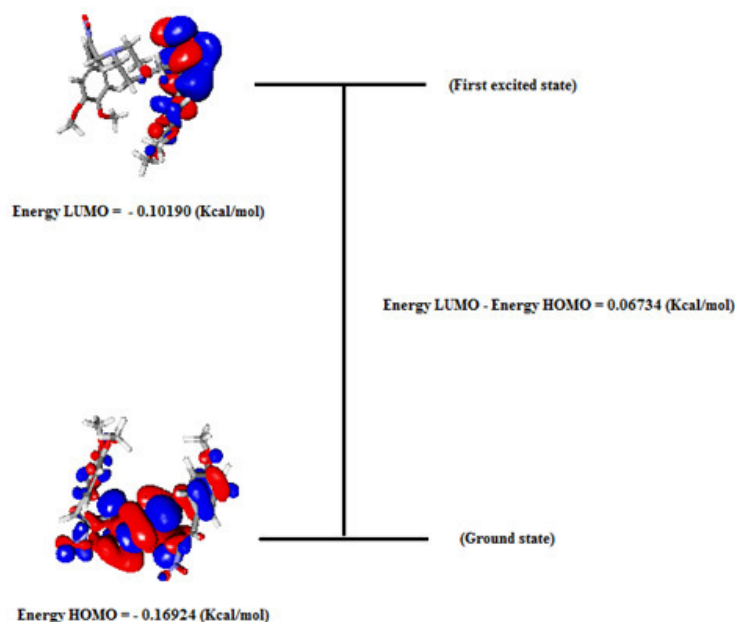


Figure 12
The Frontier molecular orbital and explicited (HOMO – LUMO) energy level gap diagram for the compound of 10g 1,4-bis((E)-3-(3,4-dimethoxyphenyl)-2-nitroallyl)piperazine.

Table 6

DFT Results of 10g 1,4-bis((E)-3-(3,4-dimethoxyphenyl)-2-nitroallyl)piperazine.

Ligand S.No	Total Energy DMol3 (Kcal/mol)	Binding Energy DMol3 (Kcal/mol)	HOMO Energy DMol3 (Kcal/mol)	LUMO Energy DMol3 (kcal/mol)	Band Gap Energy DMol3 (Kcal/mol)	Dipole Mag DMol3 (Kcal/mol)	Dipole X DMol3 (Kcal/mol)	Dipole Y DMol3 (Kcal/mol)	Dipole Z DMol3 (Kcal/mol)
10g	-1935.1606	-122.0585	-0.169242	-0.101904	0.0673375	5.541732	-1.25974	-3.88839	-3.74223

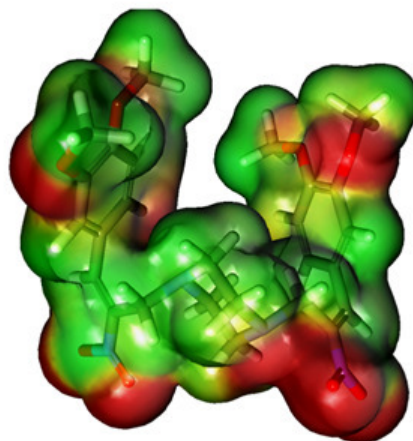


Figure 13
Molecular electrostatic potential map calculated at Dmol3properties of B3LYP function.

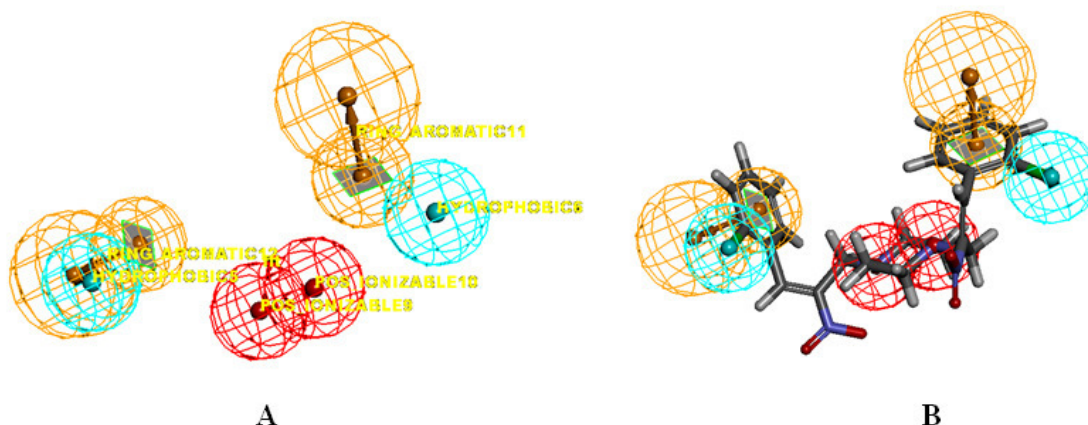


Figure 14
A - pharmacophore generation and B - Final hit compounds mapped to the best pharmacophore model, 10g1,4-bis((E)-3-(3,4-dimethoxyphenyl)-2-nitroallyl)piperazine.

The majority of quinoline drugs for example norfloxacin and ciprofloxacin having piperazine nucleus proved broad spectrum activity of urinary, gastrointestinal tracks, skin and soft tissue infection caused by either Gram- negative or Gram-positive bacteria. The novel piperazine linked chalcone derivatives proved potent antibacterial activity against *Staphylococcus aureus*, *Escherichia coli*, *Proteus vulgaris* and antifungal activity against *Aspergillus fumigatus* and *Candida albicans*.²⁶ Investigation of Antibacterial Activity of Cinnamyl Derivatives of Aryl piperazine derivatives expressed activity towards *S. longisporum* and *P. aeruginosa* that was almost as strong as that of amikacin.²⁷ In the present study, eleven novel *N,N'*-disubstituted β -branched nitroolefin piperazine derivatives and its *in-vitro* and *in-silico* work was carried out successfully. The compound 10g1,4-bis((E)-3-(3,4-dimethoxyphenyl)-2-nitroallyl) piperazine showed better ADMET results and were non-mutagenic and non-carcinogenic. The compound 10g showed low energy gap in DFT studies which also exhibited higher

antibacterial activity by both disc diffusion and MIC assays against the test bacteria.

CONCLUSIONS

The compound 10g1,4-bis((E)-3-(3,4-dimethoxyphenyl)-2-nitroallyl)piperazine showed higher ligand-receptor binding interaction with binding energy of -162.782 and also showed desirable pharmacokinetic properties and antibacterial activity. Hence, the compound 10g could be further explored for other biological activities.

ACKNOWLEDGMENT

The authors wish to thank the BIFC (Bio Informatic Facility Center), at Queen Mary's College, Ch -04, for providing infrastructure and the licenced software to carry out the project.

CONFLICT OF INTEREST

Conflict of interest declared none.

REFERENCES

1. Wyrzykiewicz E, Wendzonka MandKedzi B. Synthesis and antimicrobial activity of new (E)-4-[piperidino(4'-methylpiperidino-,morpholino-)N-alkoxy]stilbenes. Eur. J. Med. Chem. 2006 April; 41(4):519-525.
2. Kerns RJ, Rybak MJ, Kaatz G W, Vaka F, Cha R, Grucz RG. And Diwadkar VU. Structural features

- of piperazinyl-linked ciprofloxacin dimmers required for activity against drug-resistance strains of staphylococcus aureus. *Bioorg. Med. Chem. Lett.* 2003 July 7;13(13): 2109-2112.
3. Ryckebusch A, Poulain R, Maes L, Debreu-Fontaine MA, Mouray E, Grellier P. and Sergheraert C. Synthesis and in vitro and in vivo antimalarial activity of N'-(7-chloro-4-quinolyl)-1,4-bis(3-aminopropyl)piperazine derivatives. *J. Med. Chem.* 2003 January 21;46 (4):542-57.
 4. Kimura M, Masuda T, Yamada K, Mitania M, Kubota N, Kawakatsu N, Kishii K, Inazu M, Kiuchi Y, Oguchi K. and Namiki T. Novel diphenylalkylpiperazine derivatives with high affinities for the dopaminetransporter. *Bioorg. & Med. Chem.* 2003 September 1;11(18): 3953-63.
 5. Zhang Y, Rothman RB, Dersch CM, de Costa BR, Jacobson AE, Rice KC. Synthesis and Transporter Binding Properties of Bridged Piperazine Analogues of 1-{2-[Bis(4-fluorophenyl)methoxy]ethyl}-4-(3-phenylpropyl)piperazine (GBR 12909). *J. Med. Chem.* 2000 November 18;43(25):4840-49.
 6. Reviews: (a) Palomo C, Oiarbide M and Laso A. *Eur. J. Org. Chem.*, 2007 March 16; 2007(16):2561-74;
 7. Nagappan Sivakumar and Chendrasekaran Yogalakshmi. synthesis of bromo and chloro derivatives of baylis–hillman adducts. *International Journal of Advanced Research in Engineering and Technology.* 2015 Oct;10(6):01-05.
 8. Nagappan Sivakumar, Vadivelu Balasubramanian, Mavarayan Sivakumar. Synthesis of (E)-4-nitro-5-phenylpent-4-en-2-one derived from Baylis–Hillman Adduct. *International Journal of ChemTech Research.* 2017;10(1):51-4.
 9. Periyasamy Amudha, Palaniappan Matheswaran, Nagappan Sivakumar*, Vadivelu Balasubramanian. Synthesis of Novel class of (E)-N-(2-nitro-3-phenylallyl)aniline using H₂SO₄ Derived from Baylis–Hillman dduct. *International Journal of ChemTech.* 2017; 10(1): 47-50.
 10. A. A. Golovanov, V. V. Bekin, I. S. Odin, A. Yu. Chertov, O. B. Grigor'eva, and V. S. Pisareva. Nucleophilic Addition of Heterocyclic Amines to Conjugated Enyne. *Russian Journal of Organic Chemistry.* 2015 december, 51(12):1688–92.
 11. Thomas Seidensticker A, Jonas M. Vosberg A, Karoline A. Ostrowski, a and Andreas J. Vorholta. Rhodium-Catalyzed Bis-Hydroaminomethylation of Linear Aliphatic Alkenes with Piperazine. 2016 January 18;358 (4):610-21.
 12. Islam MA, Alam MM, Choudhury ME, Kobayashi N and Ahmed MU. Determination of Minimum Inhibitory Concentration (MIC) of Cloxacillin for Selected Isolates of Methicillin-Resistant Staphylococcus Aureus (MRSA) With Their Antibiogram. *Bangl. J. Vet. Med.* 2008 6;1:121–6.
 13. Khan ZK. In vitro and vivo screening techniques for bioactivity screening and evaluation, in: *Proceedings of the International Workshop. UNIDO-CDRI.* 1997;210- 11.
 14. Koska J, Spassov VZ, Maynard AJ, Yan L, Austin N, Flook PK, Venkatachalam, CM. Fully automated molecular mechanics based induced fit protein-ligand docking method. *J. Chem. Inf. Model.* 2008 September 25;48(10):1965-73.
 15. Tirado-Rives J, Jorgensen WL. Contribution of conformer focusing to the uncertainty in predicting free energies for protein-ligand binding. *J. Med. Chem.* 2006 September 12;49(20):5880-4.
 16. Spassov VZ, Flook PK, Yan L, Loofer. a molecular mechanics-based algorithm for protein loop prediction. *Protein Engineering Design and Selection.* 2008 February 1; 21(2), 91-100.
 17. Spassov VZ, Yan LA. fast and accurate computational approach to protein ionization. *Protein Science.* 2008 Nov;17(11):1955-70.
 18. Faramarzi MA, Beikmohammadi L, Shirazi FH, Shafiee A. Synthesis and antibacterial activity of new fluoroquinolones containing a substituted N-(phenethyl) piperazinemoiety. *Bioorg Med Chem Lett.* 2006 July 1;16(13):3499-503.
 19. Alireza Foroumadi, Saeed Emami, Shahla Mansouri, Azita Javidnia, Nosratollah Saeid-Adeli, Farshad HS, Abbas Shafiee. Synthesis and antibacterial activity of levofloxacin derivatives with certain bulky residues on piperazine ring. *Eur J Med Chem* 2007 July;42(7):985-92.
 20. Daisy P and Suveena S. Solutions to pharmaceutical issues for anti-cancer drugs by accord excel. *Asian journal of pharmaceutical and clinical research.* 2012 May 27;5(3):149-58.
 21. Jayakanthan M, Wadhwa G, Madhan Mohan T, Arul L, Balasubramanian P and Sundar D. Computer aided drug design for cancer-causing H-Ras P21 mutant protein. *Letterin Drug Design and Discovery.* 2009 January 1;6(7):14-20.
 22. Xia X, Maliski EG, Gallant P, Rogers D. Classification of kinase inhibitors using a Bayesian model. *J. Med. Chem.* 2004 April 8;47(18):4463-70.
 23. Levy M. Universal variational functionals of electron densities, first-order density matrices, and natural spin-orbitals and solution of the v-representability problem. *Proc. Natl. Acad. Sci. U. S. A.* 1979 December 1;76(12):6062-5.
 24. Eroglu E, Turkmen H. A DFT-based quantum theoretic QSAR study of aromatic and heterocyclic sulfonamides as carbonic anhydrase inhibitors against isozyme. CA-II. *J Mol Graph Model.* 2007 Nov; 26(4): 701–8.
 25. Ai C, Li Y, Wang Y, Li W, Dong P, Ge G, *et al.* Investigation of binding features: effects on the interaction between CYP2A6 and inhibitors. *J Comput Chem.* 2010 March 24;31(9): 1822–31.
 26. Tomar V, Bhattacharjee G, Kamaluddin, Kumar A. Synthesis and antimicrobial evaluation of new chalcones containing piperazine or 2,5-dichlorothiophene moiety *Bioorganic & Medicinal Chemistry Letters.* 2007 October 1, 17(19), 5321-24.
 27. Irena Novakovic, Jelena Penjisevic, Sukalovic V, Deana Andric, Roglic G and Sladana Kostic Rajacic. Investigation of Antibacterial Activity of Cinnamyl Derivatives of Arylpiperazine. *Arch. Biol. Sci., Belgrade.* 2012; 64(1): 15-20.